Crystallization of Block Copolymers. 1. Small-Angle X-ray Scattering Study of an ϵ-Caprolactone–Butadiene Diblock Copolymer

Shuichi Nojima,* Kazunori Kato, Satoru Yamamoto, and Tamaichi Ashida

Department of Biotechnology, School of Engineering, Nagoya University, Nagoya 464-01, Japan

Received October 30, 1991; Revised Manuscript Received December 31, 1991

ABSTRACT: The morphology formed in a crystalline–amorphous diblock copolymer, ϵ-caprolactone-*block*-butadiene (PCL-*b*-PB), has been investigated by small-angle X-ray scattering (SAXS) at various temperatures. The process of the morphology formation is also observed by time-resolved SAXS employing synchrotron radiation. Crystallization of the PCL block brings about a dramatic change in the shape of the SAXS pattern; a diffuse intensity maximum arising from the *correlation hole effect* of disordered block copolymers could be observed at the melt, while it was replaced by a strong intensity peak at a smaller angle for temperatures below T_m (melting temperature of the PCL block). The time-resolved SAXS curves revealed that the copolymer, which was quenched from the melt into a temperature below both T_m and T_s (microphase-separation temperature of the copolymer), immediately showed a sharp diffraction due to the microstructure of the copolymer, followed by a strong intensity peak at a smaller angle owing to the crystallization of the PCL block. This indicates that an energetic gain in crystallization overwhelms that in microphase separation, so that the microstructure is completely destroyed by the following crystallization of the PCL block.

Introduction

Block copolymers show a well-ordered microstructure when cast from a solvent.[1] Microsphere, cylinder, lamella, and ordered bicontinuous double diamond (OBDD) recently found[2] are commonly observed according to the block ratio within the copolymer. In these studies, amorphous blocks are certainly used in order to avoid an additional morphological complexity due to the crystallization of constituent blocks.[3-5]

In the case of crystalline–amorphous block copolymers, morphology formation is expected by crystallization, microphase separation, or a cooperative effect of these two factors, and eventually a complicated morphology will appear in the system. There are some experimental studies of such morphologies,[6-15] in which Gervais and Gallot investigated the morphology of triblock copolymers including poly(ethylene oxide) (PEO) or poly(ϵ-caprolactone) (PCL) as a crystalline block and polystyrene (PS) or polybutadiene (PB) as an amorphous block.[7-10] An alternate structure consisting of the crystalline lamella and amorphous layer was observed when the copolymer was cast from a good solvent. Cohen and co-workers have recently studied the morphology of diblock copolymers with a polyethylene block[12,14] and discussed a significant path dependence of the final morphology. That is, the morphology due to the microphase separation or crystallization is *locked* during solvent casting, and this kind of sample history substantially controls the final morphology. The theoretical approach is recently made by Di Marzio et al.,[16] Whitmore and Noolandi,[17] and Vilgis and Halperin,[18] where an equilibrium morphology of crystalline–amorphous diblock copolymers is discussed on the basis of a chain-folded lamellar model, which is thermodynamically favorable for the accommodation of the amorphous block between lamellae. In these studies, the characteristic morphology of crystalline polymers under a specific constraint (i.e., the crystalline polymer is inherently connected with an amorphous chain by a covalent bond) is mainly investigated at a thermodynamical equilibrium. Little attention is paid to the cooperative effect of crystallization and microphase separation on the process of morphology formation in such copolymer systems.

In the present study, we investigate the final morphology and the behavior of morphology formation in ϵ-caprolactone–butadiene (PCL-*b*-PB) diblock copolymers. This system was chosen because (1) the glass transition temperature (T_g) of both PB and PCL chains is low enough (below −80 °C for PB[19] and ca. −60 °C for PCL[20]), so that morphology formation will be little disturbed by the glass transition of the constituent blocks at above room temperature even without any solvent, and (2) the electron density difference is large enough between PB (291.7 e/nm^3 at 40 °C[21]) and PCL (350.3 e/nm^3 for the amorphous state at 40 °C[22] and 392.9 e/nm^3 for the perfect crystal[23]), so that the SAXS measurement is suitable to pursue the process of morphology formation in combination with a strong X-ray source. The melting behavior of the copolymer was investigated by differential scanning calorimetry (DSC). The final morphology at various temperatures ranging from room temperature to 110 °C was investigated by a conventional small-angle X-ray scattering (SAXS) technique. The process of morphology formation was also observed by time-resolved SAXS with synchrotron radiation after the copolymer was quenched from a homogeneous state into a temperature both below T_m (melting temperature of the PCL block) and T_s (microphase-separation temperature of the copolymer). The cooperative effect between crystallization and microphase separation was elucidated on the process of morphology formation of this copolymer system.

Experimental Section

1. Materials. The ϵ-caprolactone–butadiene diblock copolymers (PCL-*b*-PB) used in this study were synthesized by a successive anionic polymerization under vacuum. The butadiene monomer in toluene was first polymerized at 25 °C for 2 days with *n*-butyllithium as the initiator followed by addition of a ϵ-caprolactone monomer to synthesize the block copolymer at −20 °C for 5–15 min.[24] The butadiene monomer/initiator ratio and the reaction time of the ϵ-caprolactone monomer were adjusted to obtain copolymers with various compositions and molecular weights. We also took care to prevent depolymerization (backbiting) by the living ϵ-caprolactone end during the anionic growth of the PCL block.[25] All samples were characterized by gel permeation chromatography (GPC), and the PCL content in the copolymer was also evaluated by elementary analysis. The melting temperature of the PCL block was measured by DSC (MAC Science Model 3100) at a heating rate of 5 °C/min.

Table I shows the molecular characteristics of the samples used for the present study. All copolymers (designated by B4,

0024-9297/92/2225-2237$03.00/0

Table I
Characterization of Polymers Used in This Study

notation	polymer	source	total M_w[c]	M_w/M_n[c]	PCL:PB[d]	mp,[e] °C
B4	PCL-*b*-PB	*a*	13 700	1.19	20:80	~41
B5	PCL-*b*-PB	*a*	9 400	1.05	36:64	~41
B6	PCL-*b*-PB	*a*	12 500	1.35	45:55	~43
PCL1	PCL	SPP[b]	16 100	1.71		56.9

[a] Synthesized in our laboratory. [b] Obtained from Scientific Polymer Products, Inc., and fractionated with a benzene/*n*-heptane system. [c] Determined by GPC. [d] Determined by elementary analysis. [e] Determined by DSC.

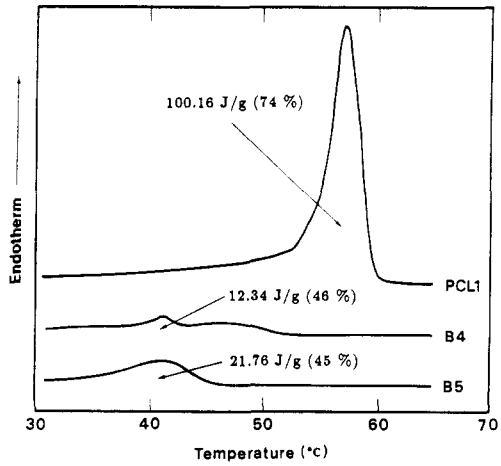

Figure 1. DSC thermograms for B4, B5, and pure PCL (M_w = 16 100) crystallized at 27 °C for 5 h. The heating rate is 5 °C/min. The melting point was defined as the temperature at which the endothermic peak was maximum. The numeral in parentheses represents the crystallinity of the PCL chain, which was evaluated from the peak area assuming that the heat of fusion for the perfect PCL crystal is 135.44 J/g.[22]

B5, and B6) show a diffuse melting endotherm with a melting temperature T_m around 42 °C (Figure 1). B4 has a microphase-separation temperature (T_s) probably below room temperature, while B5 and B6 have T_s around or above T_m judging from the plot of $1/I_{max}$ vs $1/T$.[26] Therefore, a cooperative morphology formation between microphase separation and crystallization is expected for B5 and B6, while only crystallization is expected for B4.

2. Conventional Small-Angle X-ray Scattering (SAXS) Measurement.[27,28] SAXS measurement was performed at each temperature with a pinhole collimation system and a one-dimensional position-sensitive proportional counter (PSPC) made by Rigaku Co. Nickel-filtered Cu Kα radiation (λ = 0.1542 nm) supplied from a rotating anode X-ray generator (Rigaku RU-300) operated at 50 kV and 100 mA was used. The distance between the sample and the PSPC was about 400 mm. After the SAXS intensity was corrected for the linearity and sensitivity of the PSPC and background scattering, the relative scattered intensity was obtained as a function of wavenumber s (=2 sin (θ/λ), 2θ = scattering angle). The SAXS intensity was measured after the sample was annealed in the SAXS apparatus for a long time at each temperature (T_c), which was adequately controlled by circulating water with a constant temperature. The time necessary for each measurement was 2000 s, during which the sample was kept at T_c within the fluctuation of 0.1 °C.

3. Time-Resolved SAXS Measurement with Synchrotron Radiation.[29] The process of morphology formation was observed by SAXS with synchrotron radiation. The experiment was carried out at National Laboratory for High Energy Physics, Tsukuba, Japan (Photon Factory), with small-angle X-ray equipment for solution (SAXES) installed on a Beamline BL-10C.[27,28] The storage ring was operated at an energy level of 2.5 GeV with a ring current of 250–300 mA during the period of 12 or 24 h. The SAXES employs a *point* focusing optics with a double flat monochromator followed by a bent cylindrical mirror. The incident beam intensity (with λ = 0.1488 nm) was monitored by an ionization chamber for the correction of a minor decrease of the intensity during measurements. The scattered intensity was detected with a PSPC with 512 channels, and the distance between the sample and the plane of registration was about 2000 mm. The geometry was further checked by a chicken tendon collagen, which gives a set of sharp diffractions corresponding to 65.3 nm. Details of the optics and the instrumentation are described elsewhere.[30]

The sample temperature was controlled by circulating water with a constant temperature,[27,28] by which temperature fluctuation was achieved within the range of 0.2 °C throughout the experiment. The crystallization of the PCL block was started by dropping the water temperature from a homogeneous state of the block copolymer (~55 °C) to T_c, and it took about 1 min for the sample to reach T_c. The SAXS intensity was collected as the sum of the scattered intensity during a period of 10 or 20 s from the beginning of the temperature drop, and the measurement was continued until the overall scattering profile had changed no more.

The SAXS intensity measured was corrected for the decrease of the ring current and background scattering. Since the optics of SAXES is of the *point* focusing, the scattered intensity was not corrected for the smearing effect by the finite cross section of the primary beam.[28] The SAXS curve was obtained as a function of time t after the temperature had dropped to T_c.

Results

1. Melting Temperature and Crystallinity. Figure 1 shows the DSC thermogram for the pure PCL (M_w = 16 100) and copolymers crystallized at 27 °C for 5 h. The melting endothermic curve of the copolymers is diffuse with the melting temperature T_m around 42 °C, which is about 15 °C lower than T_m of the pure PCL. A slight variation of the melting temperature can usually be observed in homopolymers crystallized from the melt or from a compatible blend according to the crystallization temperature. This change is intimately related to the lamellar thickness (or stem length in the lamella) kinetically determined under a nonequilibrium crystallization.[31] In the case of block copolymers, a large decrease of T_m (~20 °C) is reported for a block copolymer with *trans*-1,4-polyisoprene,[11] which is in conformity with the large decrease of the stem length in the lamellar crystal. The amount of this decrease in T_m is comparable with the present result and may suggest the essential difference in crystallization mechanism between block copolymers and homopolymers.[16-18]

The crystallinity of the PCL block is about 45% for B4 and B5, which is significantly less than the crystallinity of pure PCL (74%). For the crystalline–amorphous diblock copolymers such as polystyrene-*block*-polyethylene (PS-*b*-PE),[12] significant path dependence of the morphology is reported, which yields a large variation in the crystallinity. This is attributed to a high molecular weight (M_{total} > 100 000) and a high glass transition temperature (T_g of the PS block is about 100 °C) of the PS-*b*-PE copolymer. The present PCL-*b*-PB copolymers, on the other hand, have a relatively low molecular weight and low glass transition temperatures, so that they have enough mobility so as to take a favorable morphology even without any solvent.

2. SAXS Curve of the Final Morphology. Figure 2 shows the SAXS curves from B5 annealed at various temperatures indicated. At temperatures above T_m, a diffuse intensity maximum at $s \sim 0.1$ nm^{-1} is observed, which grows in intensity with decreasing temperature, with the angular position of the peak intensity being constant. This scattering maximum can be generally observed for block copolymers at a disordered state and is attributed to the correlation hole effect of the homogeneous copolymer.[32] In the SAXS curves below T_m, on the other hand, a strong intensity peak at $s \sim 0.05$ nm^{-1} appears, which shifts toward a smaller angle with the annealing temperature

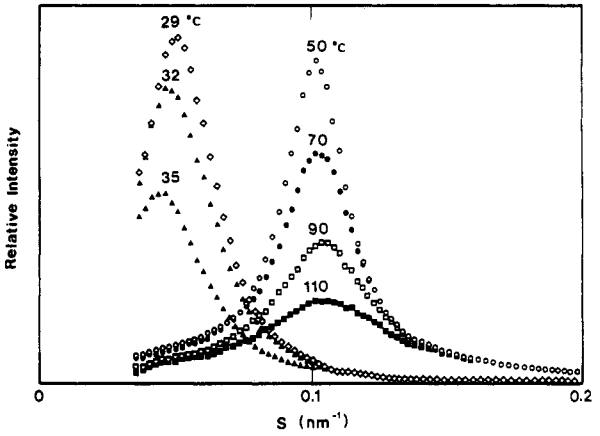

Figure 2. Relative intensity plotted against wavenumber s for B5 at various temperatures indicated. The scattering curves for 50, 70, 90, and 110 °C are enlarged in magnitude by a factor of ca. 20 for clarity.

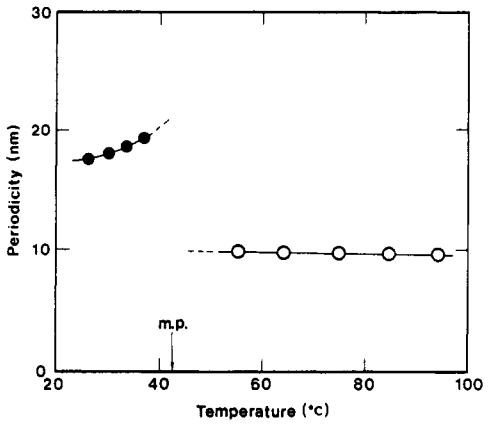

Figure 3. Periodicity (or long spacing) plotted against temperature for B5. The closed circles were evaluated from the scattering peak due to the crystallization and the open circles from the diffuse scattering due to the correlation hole effect. The melting temperature of the PCL block is represented by the arrow.

approaching to T_m. The angular position of the peak intensity for B6 is almost the same as that of B5 at temperatures below and above T_m, while the peak angle for B4 is too small at temperatures below T_m to be detected with our SAXS apparatus. The dramatic change of these SAXS curves with the block ratio reflects the characteristic morphology of crystalline–amorphous block copolymers, the details of which are intimately dependent on the block ratio. Figure 3 shows the periodicity or long spacing L calculated from the angular position of the diffuse peak intensity above T_m and of the strong peak intensity below T_m. As expected from Figure 2, L is discontinuous at T_m. The effect of the microphase separation (for B5 and B6) on the final morphology cannot be observed in Figures 2 and 3, and we will find later that the microphase separation appears on the process of morphology formation.

A combination of microscopic and scattering techniques is powerful for a quantitative determination of the unknown structure.[33] Therefore, the definite morphology of the present copolymers after crystallization is difficult to determine uniquely by the SAXS technique. In the previous studies with crystalline–amorphous diblock copolymers,[6-14] not only lamellar structure but also cylindrical and micellar structures were observed, which are significantly dependent on the block ratio in the copolymer. Theoretical treatment by Vilgis and Halperin[18] also assumes the lamellar, cylindrical, and micellar structures for the shape of crystalline aggregates and evaluates the block-length dependence of the characteristic

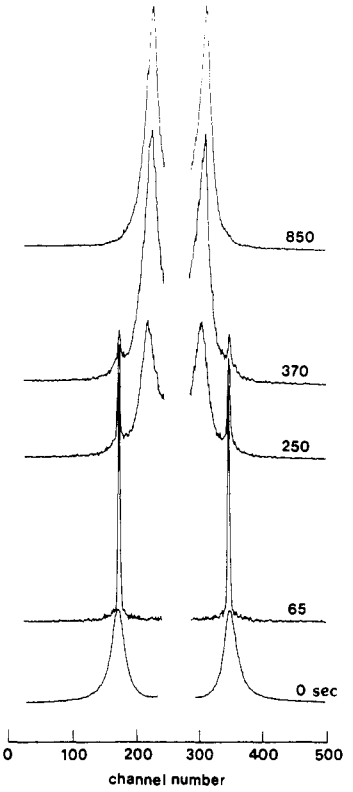

Figure 4. Time-resolved SAXS curve plotted against channel number for B5 quenched from ca. 55 °C into T_c = 28.7 °C. Channel number 258 corresponds to the zero angle, and the SAXS curve is symmetrical against this channel. The numerals in the figure represent the time after the sample was quenched from the melt. The SAXS curve for 0 s is the accumulation during the period of 300 s, and the others are those of 10 s.

size. In the present case, the crystalline block does not exceed 50% in fraction, so that the lamellar thickness should be smaller than the amorphous layer thickness if an alternate structure of the lamella and amorphous layer is assumed. When this lamellar structure is not energetically favorable, the micellar structure, in which the PCL lamella is surrounded by a large volume of amorphous PB chains, will appear. The long spacing, in this case, represents the neighboring distance between micelles[34] and may have an extremely large value compared with the case of ordinary crystalline polymers. It is necessary to elucidate the morphology by the other technique, for example, by electron microscopy.

3. Time-Resolved SAXS Curves. Figure 4 shows the time evolution of the SAXS curve measured with B5 quenched from a homogeneous melt (ca. 55 °C) into 28.7 °C and Figure 5 that measured with B4 quenched into 21.0 °C. At the melt (t = 0 s), there appears a diffuse scattering maximum due to the correlation hole effect of the homogeneous block copolymer.[32] In Figure 4, this scattering maximum is replaced by a sharp diffraction just after quenching (65 s), with the angular position of the maximum intensity being slightly smaller than that from the melt. The diffraction comes from the microstructure of the block copolymer; B5 has T_s around T_m, so that the microphase separation takes place at 28.7 °C. In Figure 4, there appears a second intensity maximum at a smaller angle (250 s), this maximum intensity grows with time, and the sharp diffraction simultaneously reduces in intensity and finally disappears (850 s). The second intensity maximum is identical to that observed by the conventional SAXS technique (Figure 2) below T_m judging from its feature and the angular position of the peak intensity. For the B4 sample, on the other hand, T_s is

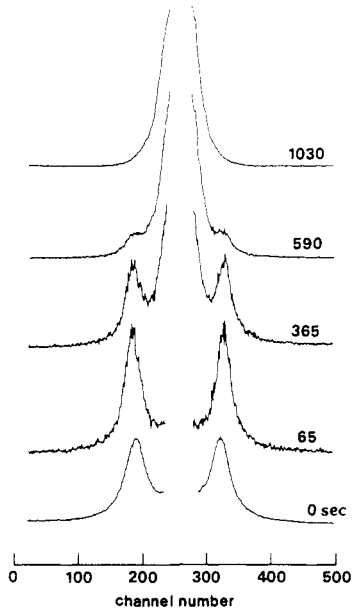

Figure 5. Time-resolved SAXS curve plotted against channel number for B4 quenched from ca. 55 °C into T_c = 21.0 °C. The SAXS curve for 0 s is the accumulation during the period of 300 s, and the others are those of 10 s. The ordinate is not the same as that of Figure 4.

lower than room temperature, so that no sign of the microphase separation has appeared during the morphological transition. That is, there appears a strong scattering at a lower angle after quenching (365 s) due to the crystallization of the PCL block, probably the peak being located inside the beam stop. The strong scattering intensity grows with time, and the diffuse intensity maximum decreases and finally disappears (1030 s). The following facts can be extracted from Figures 4 and 5: (1) The induction time of the microphase separation cannot be detected, and the copolymer presents the microstructure as soon as it is quenched below T_g. The induction time of crystallization is, on the other hand, extremely long. This time is also much longer than the induction time of the crystallization for pure PCL homopolymer at the same temperatures.[27] The essential difference in the induction time suggests a difference in the mechanism between microphase separation and crystallization at a molecular level. (2) The crystallization of the PCL block occurs spontaneously from the microstructure formed in the system; that is, the energetic gain in the crystallization overwhelms that in the microphase separation, so that the microstructure is completely destroyed by the following crystallization. Morphological freezing by the microphase separation could not be observed in the present copolymers, though such freezing is reported for some crystalline–amorphous block copolymers such as polyethylene-*block*-polystyrene[12] during solvent-casting, which is attributed to the glass transition of the amorphous block or low mobility due to the high molecular weight of copolymers. In our copolymers, however, the crystalline and amorphous blocks have enough mobility even in the microstructure owing to the relatively low molecular weight, so that it seems possible to take a morphological transition according to the free-energy reduction of the system. Once the crystallization occurs, no further morphological change is expected because of freezing of the PCL block in the crystal.

4. Time Dependence of the SAXS Profile. Figure 6 shows the angular position of the peak intensity for B6 at T_c = 26.5 °C. The closed symbol represents the major peak at each t. The diffraction peak appears at $L \sim 12$ nm immediately after quenching, and the second peak due to the crystallization follows at $L \sim 20$ nm. During the morphology formation, both angular positions of the peak intensity are strictly constant, suggesting the morphology is not further distorted, as usually observed at the early stage in the crystallization of homopolymers owing to the rearrangement of the lamellar structure.[35]

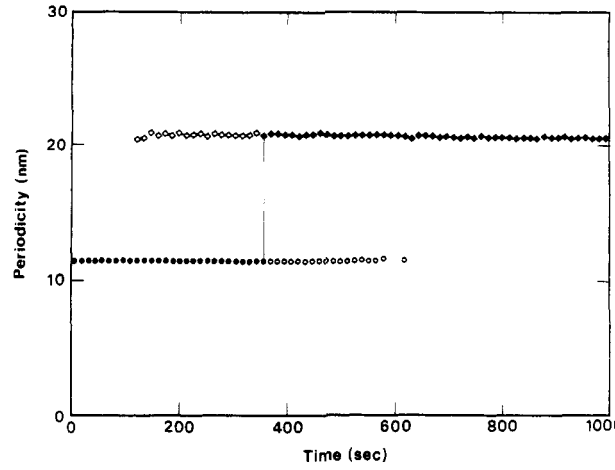

Figure 6. Periodicity (or long spacing) due to the microphase separation (circle) and crystallization (diamond) plotted against time for B6 at T_c = 26.5 °C. The closed symbols represent the major peak at every time.

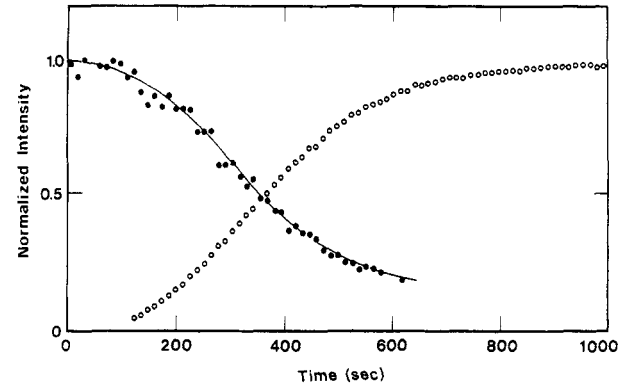

Figure 7. Normalized intensities for the microphase separation (●) and crystallization (○) plotted against time for B6 at T_c = 26.5 °C. The curves meet each other at half of their maximum intensities.

Figure 7 shows the time dependence of the normalized maximum intensities of the sharp diffraction (at $s \sim 0.08$ nm^{-1}) and strong scattering (at $s \sim 0.05$ nm^{-1}) for B6 at T_c = 26.5 °C. The intensity of the diffraction peak decreases with an inverse sigmoidal shape, while the strong scattering increases with a sigmoidal shape, and they coincide with each other when both normalized intensities approximately equal 0.5. A similar change could be obtained for every sample (B5 and B6) at all temperatures investigated. The time dependence of the peak intensity due to the crystallization is reminiscent of that for the PCL homopolymer[27] though the process is extremely expanded in this case. The shape, however, makes us speculate that the whole process of the morphology formation is substantially controlled by the crystallization of the PCL block. If the microstructure significantly affects the following crystallization process or a new cooperative effect functions between the microphase separation and crystallization, the time dependence of the maximum intensity should be different in the shape from the sigmoidal curve.

5. Temperature Dependence of the SAXS Profile. Figure 8 shows the temperature dependence of the half-

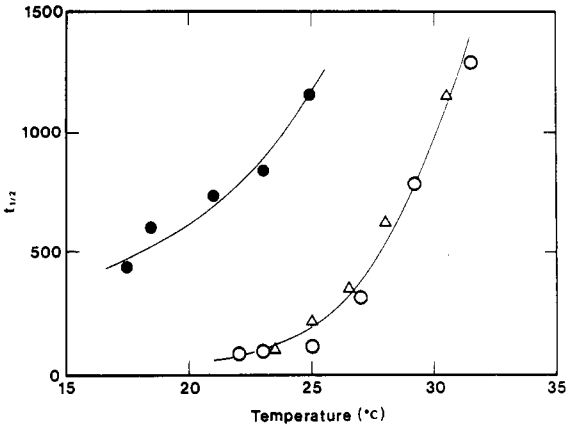

Figure 8. Half-time of crystallization, $t_{1/2}$, plotted against temperature for B4 (●), B5 (○), and B6 (△).

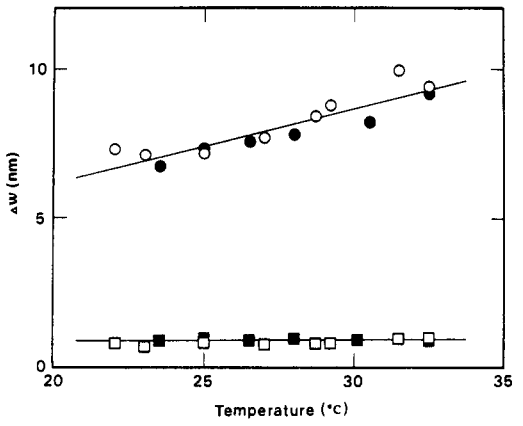

Figure 9. Half-width of the maximum intensities for B5 (open symbol) and B6 (closed symbol) plotted against temperature. Squares were obtained from the diffraction peak due to the microphase separation and circles from the scattering peak due to the crystallization.

time of morphology formation $t_{1/2}$, that is, the time necessary to reach half of the final peak intensity due to the crystallization. $t_{1/2}$ is approximately identical to the time when the diffraction peak becomes half in intensity. The magnitudes of $t_{1/2}$ for B5 and B6 are almost the same at the same temperatures, while $t_{1/2}$ for B4 is extremely large compared with that of B5 or B6 at the same temperatures. A plausible explanation of this difference is that, in the case of B5 and B6, the microstructure already appears before crystallization of the PCL block, and the resultant aggregation of the PCL chain promotes the following crystallization. That is, the microphase separation accelerates the following crystallization. In the case of B4, on the other hand, the system is homogeneous and PCL blocks are dispersed in the system just before crystallization, so that it takes longer time for the PCL chain to gather each of its blocks to make crystallites. The above speculation should be confirmed by the accumulation of the experimental data, because the difference in the molecular weight or the block ratio may be simply responsible for the time dependence of $t_{1/2}$ shown in Figure 8.

Figure 9 shows the temperature dependence of the peak width at the half-intensity of both maxima for B5 and B6, which represents the degree of structural regularity. The peak width for the diffraction is small and constant irrespective of temperature, indicating that the microstructure is extremely regular and almost independent of temperature. The peak width for the crystalline morphology is, on the other hand, very large and increases slightly with increasing temperature, suggesting that the

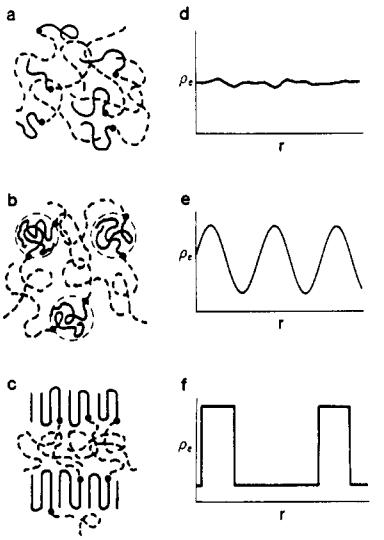

Figure 10. Schematic illustration of the morphology (a–c) and electron density profile (d–f) during phase transition of the present copolymer. The copolymer in a homogeneous state (a) changes into a micellar structure (b) just after quenching and finally into an alternate structure consisting of lamellae and amorphous layers (c). In parts d–f, the ordinate is the electron density ρ_e and the abscissa is the distance r.

lamella and/or amorphous layer have a wide distribution in thickness like the lamellar crystal found in the homopolymer. In the crystallization of block copolymers, the amount of chain folding or the lamellar thickness is predicted to be determined only by a thermodynamic balance between the crystalline and amorphous regions; in contrast, chain folding appears kinetically for homopolymer crystallization. Figure 9 may suggest that, in the present case, the kinetic factor still intervenes in the morphology formation on the crystallization of the PCL block; that is, the final morphology is not in a thermodynamical equilibrium.

Discussion

The morphology of a crystalline–amorphous diblock copolymer, ϵ-caprolactone-*block*-butadiene (PCL-*b*-PB), was investigated by small-angle X-ray scattering (SAXS) at temperatures below and above the melting point (T_m) of the PCL block. A dramatic change in the shape of the SAXS curve could be observed around T_m, suggesting morphology formation by the crystallization of the PCL block. The angular position of the peak intensity is significantly dependent on the block ratio in the copolymer. When this PCL-*b*-PB copolymer was quenched from a homogeneous melt into temperatures below T_m and T_s (microphase-separation temperature of the copolymer), the time evolution of the SAXS curve revealed that (1) the induction time of microphase separation could not be observed, while that of crystallization was extremely long, and (2) the microstructure was completely destroyed by the following crystallization of the PCL block. *Freezing* of the morphology could not be observed owing to the formation of the microstructure.

The whole morphological transition observed with B5 or B6 is illustrated in parts a–c of Figure 10 when the copolymer is quenched from the melt into temperatures both below T_s and T_m. In the transition with B4, the morphology shown in Figure 10b does not appear. The disordered melt (Figure 10a) changes into one of the microstructures just after the copolymer is quenched. This process is spontaneously controlled by the diffusion of whole molecules with no induction time. Hashimoto et al., for example, observed a fast order–disorder transition

(less than 30 s) when an ordered polystyrene-*block*-polybutadiene diblock copolymer in a solvent was brought into a disordered temperature.[36,37] Connell et al. also analyzed the small-angle neutron scattering data immediately after the concentrated solutions of a polystyrene-*block*-polyisoprene copolymer were quenched into an ordered state.[38] Although a micellar structure is depicted in Figure 10b, the present copolymers may have a cylindrical or lamellar structure judging from the block ratio in the copolymer.[39] In any case, the present microstructure will be extremely regular, because it gives the sharp diffraction shown in Figure 4, as is the case of the usual amorphous–amorphous diblock copolymers. The boundary between the two phases should be diffuse owing to the weak segregation between the two blocks. The electron density profile of this structure is illustrated in Figure 10e, and this is the reason why higher order diffractions could not be observed in Figure 4.[40] The annealing of the B6 sample at a temperature above T_m and below T_g for more than 24 h does not bring any change in the SAXS curve, indicating slow variation of the boundary profile.

The crystallization process presents a finite induction time because it involves a nucleation mechanism. In Figure 10c, the final morphology is illustrated as an alternate structure of the lamella and amorphous layer. The electron density profile at the interface between the two phases should be sharp (Figure 10f), but the thicknesses of each layer will be widely distributed from the SAXS peak width shown in Figure 9, which is comparable with the usual SAXS peak observed with crystalline homopolymers. Theories for the crystallization of block copolymers predict that the number of chain folding is strictly determined under a thermodynamical equilibrium,[16-18] which may be attained by a careful solvent-casting method. The SAXS curve shown in Figures 4 and 5, therefore, may suggest the nonequilibrium morphological transition; that is, the kinetic factor intervenes into the crystallization process and dominantly determines the final morphology in the system. This fact is also supported by a large distribution of the peak width shown in Figure 9. A comparison between morphologies formed by the solvent-casting method and the present quenching method is currently being carried out.

An interesting fact found in the time-resolved SAXS curve is that the time when the diffraction peak becomes half of the intensity is almost the same as the time when the peak due to the crystallization becomes half of the final intensity, as shown in Figure 7. This indicates that the morphological transition occurs directly from the microstructure into the crystalline morphology, and there appears no third phase (for example, disordered phase) during the transition. That is, once the nucleus has formed in the PCL domain, the system changes steadily toward the crystalline morphology according to the free-energy reduction, during which a large-scale rearrangement or decomposition of the existing microstructure does not occur.

The SAXS results tell us no specific morphology formed in the system. Especially, it is interesting to know the morphology by a visual technique such as an electron microscope before and after the PCL block crystallizes. This will also give additional information about the mechanism of morphology formation in crystalline–amorphous diblock copolymers. This study is also currently being carried out and will soon appear.

Acknowledgment. We thank the staff of the Workshop for Experimentation and Practice, School of Engineering, Nagoya University, for making sample holders to perform the time-resolved SAXS experiment. This work was supported in part by a grant of the Association for the Progress of New Chemistry (ASPRONC) and has been performed under the approval of the Photon Factory Program Advisory Committee (Proposal Nos. 90-061 and 91-245).

References and Notes

(1) Molau, G. In *Block Copolymers*; Aggarwal, S., Ed.; Plenum Press: New York, 1970; p 79.
(2) Hasegawa, H.; Tanaka, H.; Yamasaki, K.; Hashimoto, T. *Macromolecules* **1987**, *20*, 1651.
(3) Bates, F. S. *Science* **1991**, *251*, 898.
(4) Legge, N. R., Holden, G., Schroeder, H. E., Eds. *Thermoplastic Elastomers*; Hanser Publishers: New York, 1987.
(5) Wignall, G. D., Crist, B., Russell, T. P., Thomas, E. L., Eds. *Scattering, Deformation and Fracture in Polymers*; Materials Research Society: Pittsburgh, PA, 1987; Vol. 79.
(6) Hirata, E.; Ijitsu, T.; Soen, T.; Hashimoto, T.; Kawai, H. *Polymer* **1975**, *16*, 249.
(7) Gervais, M.; Gallot, B. *Makromol. Chem.* **1977**, *178*, 1577.
(8) Gervais, M.; Gallot, B. *Polymer* **1981**, *22*, 1129.
(9) Gervais, M.; Gallot, B.; Jerome, R.; Teyssie, P. *Makromol. Chem.* **1981**, *182*, 989.
(10) Herman, J. J.; Jerome, R.; Teyssie, P.; Gervais, M.; Gallot, B. *Makromol. Chem.* **1981**, *182*, 997.
(11) Zemel, I. S.; Corrigan, J. P.; Woodward, A. E. *J. Polym. Sci.* **1989**, *B27*, 2479.
(12) Cohen, R. E.; Cheng, P. L.; Douzinas, K.; Kofinas, P.; Berney, C. V. *Macromolecules* **1990**, *23*, 324.
(13) Veith, C. A.; Cohen, R. E.; Argon, A. S. *Polymer* **1991**, *32*, 1545.
(14) Douzinas, K. C.; Cohen, R. E.; Halasa, A. F. *Macromolecules* **1991**, *24*, 4457.
(15) Ishikawa, S.; Ishizu, K.; Fukutomi, T. *Polym. Commun.* **1991**, *32*, 374.
(16) Di Marzio, E. A.; Guttman, C. M.; Hoffmann, J. D. *Macromolecules* **1980**, *13*, 1194.
(17) Whitmore, M. D.; Noolandi, J. *Macromolecules* **1988**, *21*, 1482.
(18) Vilgis, T.; Halperin, A. *Macromolecules* **1991**, *24*, 2090.
(19) Dainton, F. S.; Evans, D. M.; Hoare, F. E.; Melia, T. P. *Polymer* **1962**, *3*, 297.
(20) Koleske, J. V.; Lundberg, R. D. *J. Polym. Sci., Polym. Phys. Ed.* **1969**, *7*, 795.
(21) Rigby, D.; Roe, R. J. *Macromolecules* **1986**, *19*, 721.
(22) Crescenzi, V.; Manzini, G.; Calzolari, G.; Borri, C. *Eur. Polym. J.* **1972**, *8*, 449.
(23) Chatani, Y.; Okita, Y.; Tadokoro, H.; Yamashita, Y. *Polym. J.* **1970**, *1*, 555.
(24) Nojima, S.; Wang, D.; Ashida, T. *Polym. J.* **1991**, *23*, 1473.
(25) Ito, K.; Yamashita, Y. *Macromolecules* **1978**, *11*, 68.
(26) Nojima, S.; Roe, R. J. *Macromolecules* **1987**, *20*, 1866.
(27) Nojima, S.; Tsutsui, H.; Urushihara, M.; Kosaka, W.; Kato, N.; Ashida, T. *Polym. J.* **1986**, *18*, 451.
(28) Nojima, S.; Kato, K.; Ono, M.; Ashida, T., to be submitted for publication in *Macromolecules*.
(29) Gehrke, R. *Top. Curr. Chem.* **1989**, *171*, 111.
(30) Ueki, T.; Hiragi, Y.; Kataoka, M.; Inoko, Y.; Amemiya, Y.; Izumi, Y.; Tagawa, H.; Muroga, Y. *Biophys. Chem.* **1985**, *23*, 115.
(31) Wunderlich, B. *Macromolecular Physics*; Academic Press: London, 1980; Vol. 3.
(32) de Gennes, P.-G. *Scaling Concepts in Polymer Physics*; Cornell University Press: Ithaca, NY, 1979.
(33) Thomas, E. L. In *Structure of Crystalline Polymers*; Hall, I. H., Ed.; Elsevier: London, 1984; p 79.
(34) Nojima, S.; Roe, R. J.; Rigby, D.; Han, C. C. *Macromolecules* **1990**, *23*, 4305.
(35) Elsner, G.; Zachmann, H. G.; Milch, J. R. *Makromol. Chem.* **1981**, *182*, 657.
(36) Hashimoto, T.; Kowsaka, K.; Shibayama, M.; Suehiro, S. *Macromolecules* **1986**, *19*, 750.
(37) Hashimoto, T.; Kowsaka, K.; Shibayama, M.; Kawai, H. *Macromolecules* **1986**, *19*, 754.
(38) Connell, J. G.; Richards, R. W.; Rennie, A. R. *Polymer* **1991**, *32*, 2033.
(39) Herman, D. S.; Kinning, D. J.; Thomas, E. L.; Fetters, L. J. *Macromolecules* **1987**, *20*, 2940.
(40) Hashimoto, T.; Tsukahara, Y.; Kawai, H. *Polym. J.* **1983**, *10*, 699.

Registry No. PCL-*b*-PB (block copolymer), 108564-22-3.